# Apoptotic Cell Imaging Using Phosphatidylserine-Specific Receptor-Conjugated $Ru(bpy)_3^{2+}$-Doped Silica Nanoparticles**

*Se Won Bae, Min Sun Cho, A Reum Jeong, Bo-Ra Choi, Dong-Eun Kim, Woon-Seok Yeo,* and Jong-In Hong**

Apoptosis, or programmed cell death, is a normal physiological process that occurs during embryonic development; the process plays an important role in maintaining tissue homeostasis.[1] Defective apoptosis can lead to several pathological conditions, such as neurodegenerative disorders, cardiovascular diseases, and cancers.[2] Diagnosis of apoptosis is therefore of great importance for the early determination of therapy efficiency and the evaluation of disease progression. Traditional intracellular methods for detecting apoptosis are based on changes in caspase activity and cytoplasmic compartments.[3] A popular extracellular method for the detection of apoptosis involves monitoring of the distribution of phospholipids on the cell surface.[4] In particular, phosphatidylserine (PS), which usually constitutes less than 10% of the total phospholipids in cell membranes, plays an important role in phospholipid scrambling that occurs during the early stages of apoptosis.[5] The appearance of PS on the outer leaflet of cell membranes is a universal indicator of the initial stage of apoptosis.[6] The most popular method for detecting PS on the cell surface involves the use of annexin V (AnxV), which is a calcium-dependent 35 kDa PS-binding protein.[7] The use of dye-labeled AnxV simplifies the method and makes it effective for the detection of apoptotic cells. However, this method is expensive and has some technical limitations. For example, it has been reported that AnxV can associate with membrane surfaces containing the by-product of lipid peroxidation.[8] Moreover, the 2.5 mM extracellular calcium required for complete PS binding can give rise to false-positive signals because most animal cells have a calcium-dependent scramblase that can transport PS from the inner leaflet to the outer leaflet of the cell membrane.[9] Furthermore, AnxV may not have the chemical stability required for high-throughput drug screening and in vivo imaging of dying tissues.[10] Hence, it is desirable to replace dye-labeled AnxV by a simple fluorescent substance that is cost effective, highly sensitive, fast binding, and calcium independent.

The Zn(II)–di-2-picolylamine complex (Zn(II)–DPA) is a suitable alternative that can be used to detect the phosphate moiety in PS. Smith et al. reported a Zn(II)–DPA-based fluorescent PS sensor for apoptotic cell imaging and Tung et al. reported a Zn(II)–DPA-conjugated peptide-based nanosensor for the same purpose.[11] The X-ray crystal structure of the AnxV–glycerophosphoserine complex[12] suggests that a synthetic Zn(II)–DPA complex with an appropriate charge, geometry, and spatial orientation may selectively bind to PS in preference to various animal-cell-membrane phospholipids, such as phosphatidylcholine (PC), phosphatidylethanolamine (PE), and sphingomyelin (SM). Previously, we have reported phenoxo-bridged Zn(II)–DPA complex (pbZn(II)–DPA)-based chemosensors that selectively detect pyrophosphate or diphosphate-containing biomolecules in a wide pH range (6.5 – 8.3).[13] We hypothesize that pbZn(II)–DPA can assume a preorganized rigid structure for cooperative binding to the anionic phosphate and carboxylate moiety of PS and detect PS in the presence of other zwitterionic phospholipids (PC, PE, and SM). As shown in Figure 1, PS has two anionic groups that cooperatively bind to four zinc coordination sites of pbZn(II)–DPA, while other phospholipids are weakly bound to pbZn(II)–DPA due to the absence of the carboxylate group, which facilitates tight binding with pbZn(II)–DPA, and the electrostatic repulsion between Zn(II) and the ammonium cation of the phospholipids. In this Communication, we report our findings on (i) the selective binding of pbZn(II)–DPA to PS in preference to other phospholipids and (ii) the fluorescent imaging of apoptotic cells by use of pbZn(II)–DPA conjugated with tris(2,2'-bipyridyl) ruthenium(II)-doped silica nanoparticles (RSNPs).

[*] S. W. Bae, M. S. Cho, A. R. Jeong, Prof. J.-I. Hong
Department of Chemistry
Seoul National University
Seoul 151-747 (Republic of Korea)
E-mail: jihong@snu.ac.kr
B.-R. Choi, Prof. D.-E. Kim, Prof. W.-S. Yeo
Department of Bioscience and Biotechnology
Konkuk University
Seoul 143-701 (Republic of Korea)
E-mail: wsyeo@konkuk.ac.kr

[**] This work was supported by the NRF grant funded by the MEST (No. 2009-0080734), and a grant from Industrial Technology Development, Ministry of Knowledge Economy (10032113), Republic of Korea, and BK 21 fellowships awarded to S.W.B., M.S.C., and A.R.J.

Supporting Information is available on the WWW under http://www.small-journal.com or from the author.

DOI: 10.1002/smll.201000564

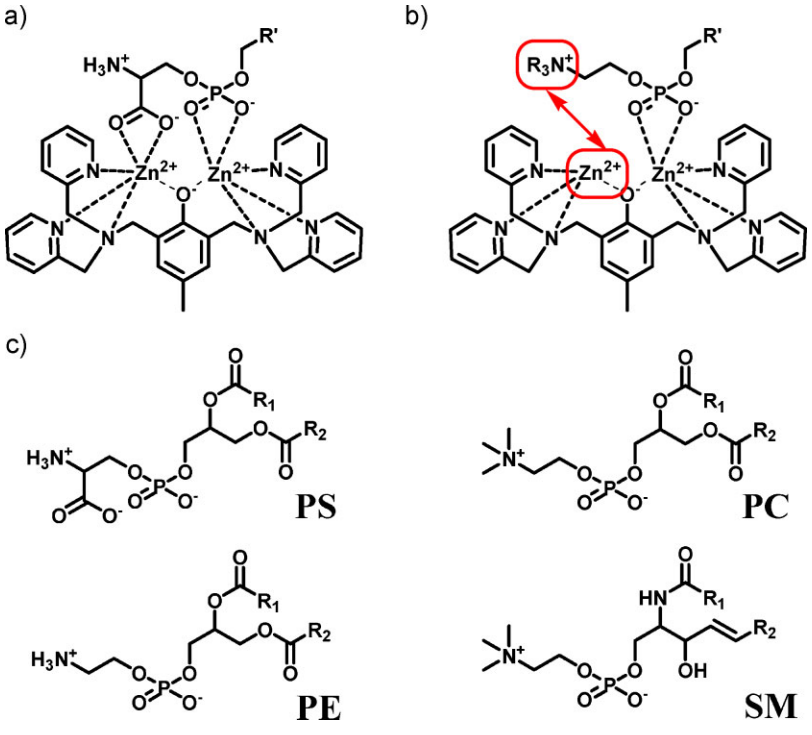


**Figure 1.** Proposed binding mode of pbZn(II)–DPA to a) PS and b) PC, PE, and SM. The red arrow indicates charge repulsion between two cations. c) Chemical structures of PS, PC, PE, and SM.

To demonstrate the preferential binding ability of pbZn(II)–DPA to PS as compared to the ability to bind to PC, we prepared unilamellar vesicles comprised of PS and PC and measured the change in the fluorescence intensity upon the addition of the vesicles to 1·2Zn in 4-(2-hydroxyethyl)-1-piperazineethanesulfonic acid (HEPES) buffer (10 mM, pH 7.4; Figure 2). The fluorescence intensity of 1·2Zn remained unchanged when treated with zwitterionic PC vesicles. However, the addition of anionic vesicles comprising PC/PS (50:50) resulted in a twelve-fold enhancement in the fluorescence intensity; the addition of vesicles containing 10 mol% PS also resulted in an eight-fold increase in the fluorescence intensity. The increase in the fluorescence intensity upon treatment with PS-containing vesicles is attributed to the weakening of the bond between the phenolate oxygen atom and Zn(II) in 1·2Zn, which results from the strong coordination of the four carboxylate and phosphate oxygen atoms on PS to the two Zn(II) ions. This in turn increased the negative charge on the phenolate oxygen atom, which resulted in more extended conjugation through the π-electron system.

After confirming that pbZn(II)–DPA selectively detects PS in a solution, we assessed its ability to sense and image apoptotic cells. Jurkat T cells were treated with camptothecin for the induction of apoptosis. They were then costained with 1·2Zn and AnxV–fluorescein-isothiocyanate (FITC) with identical concentrations (10 μM), respectively, and rinsed with culture media. As shown in Figure 3, AnxV–FITC-positive cells were also found to be positive to 1·2Zn. The merged image reveals that both 1·2Zn and AnxV–FITC were colocalized on the cell surface, as expected if they were to bind to PS.

To realize multivalent binding and fluorescence-signal amplification, we attached multiple pbZn(II)–DPAs to RSNPs. We used RSNPs containing a large number of tris(2,2'-bipyridyl) ruthenium(II) fluorophores in the silica matrix. Such RSNPs produce amplified fluorescence emission, unlike a single organic fluorescent dye.[14] In addition, the low toxicity of RSNPs and the possibility of carrying out surface modifications of RSNPs to incorporate synthetic receptors by well known methods make RSNPs attractive for use in various applications, such as cell imaging (Scheme 1). For details of the synthesis, characterization, and cytotoxicity of PS-specific receptor-conjugated RSNPs (RSNPpbZn(II)–DPAs), see the Supporting Information.

To verify the selectivity of RSNPpbZn(II)–DPA to PS in preference to PC and PE, we mixed aqueous solutions of RSNPpbZn(II)–DPA with PC, PE, and PS in $CHCl_3$. As shown in Figure 4, in the case of PC and PE in $CHCl_3$, fluorescence was observed in the upper (aqueous) layer, indicating the presence of RSNPpbZn(II)–DPA. However, in the case of PS in $CHCl_3$, RSNPpbZn(II)–DPA moved to the lower ($CHCl_3$) layer, implying the occurrence of complexation between RSNPpbZn(II)–DPA and PS. The translocation of RSNPpbZn(II)–DPA from the aqueous solution to $CHCl_3$ was further confirmed by the decrease in the fluorescence of the aqueous solution with an increase in the concentration of PS in $CHCl_3$ from 0 to 500 μM.

The fidelity of RSNPpbZn(II)–DPA to differentiate apoptotic cells from viable cells was examined by fluorescence-activated cell sorting (FACS) of Jurkat T cells. Cells were harvested and resuspended to form a suspension containing $10^5$ cells $mL^{-1}$. 1 mL of the cell suspension was placed on a well plate and 10 μM of the apoptosis inducer (camptothecin) was added. The plate was incubated for 4 h. Finally, RSNPpbZn(II)–DPA was added to the cell suspension and the suspension was incubated for 15 min. The cells were then collected and washed. The fluorescence histogram of cells before and after apoptosis induction shows an enhancement in the fluorescence intensity after camptothecin treatment (Figure 5a). Next, we examined the specificity of RSNPpbZn(II)–DPA for apoptotic cells. Cells were incubated with camptothecin for 30 min to produce evenly distributed populations of living, apoptotic, and dead cells. The whole population of the three types of cells was treated with RSNPpbZn(II)–DPA and trypan blue. Trypan blue is a well known DNA-intercalating dye used in cell-viability tests but it cannot distinguish between necrotic and apoptotic cells.[15] The cells were then washed and analyzed by FACS (Figure 5b). The yellow circle indicates living cells, whose presence is evidenced by the low fluorescence intensity of both RSNPpbZn(II)–DPA and trypan blue. RSNPpbZn(II)–DPA clearly discriminated between necrotic and apoptotic

  

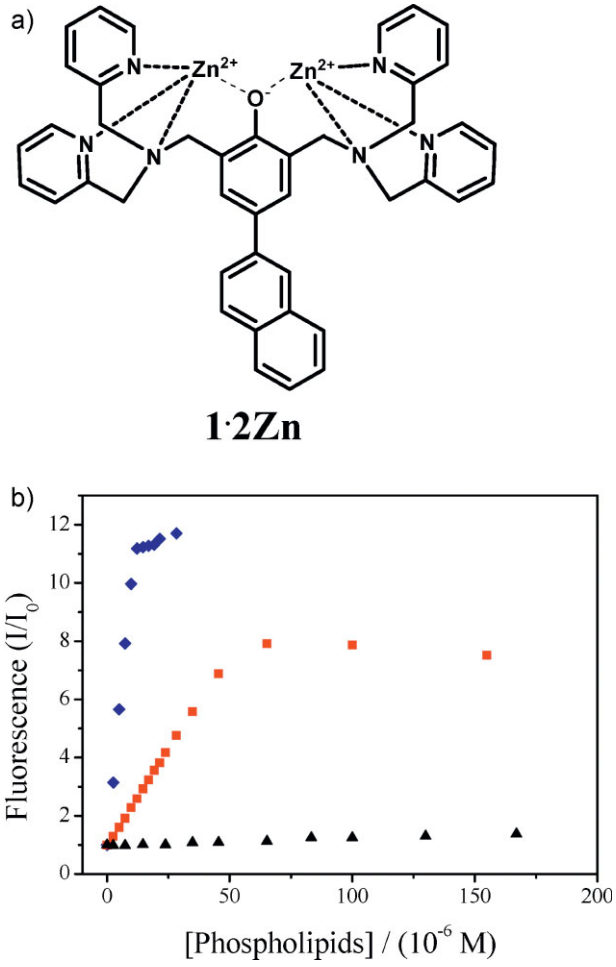


**Figure 2.** a) Chemical structure of 1·2Zn. b) Change in fluorescence intensity $I/I_0$ (excitation: 310 nm; emission: 450 nm) of 1·2Zn (5 μM) in HEPES buffer (10 mM, pH 7.4) upon addition of phospholipid vesicles comprising PC/PS (50:50, lozenges), PC/PS (90:10, squares), and 100% PC (triangles).

cells (two cell populations), as evident from the blue and red circles. However, trypan blue could not distinguish apoptotic cells (red) from necrotic cells (blue), both of which showed high fluorescence intensities when treated with the stain. Necrotic or dead cells have a highly anionic cell surface

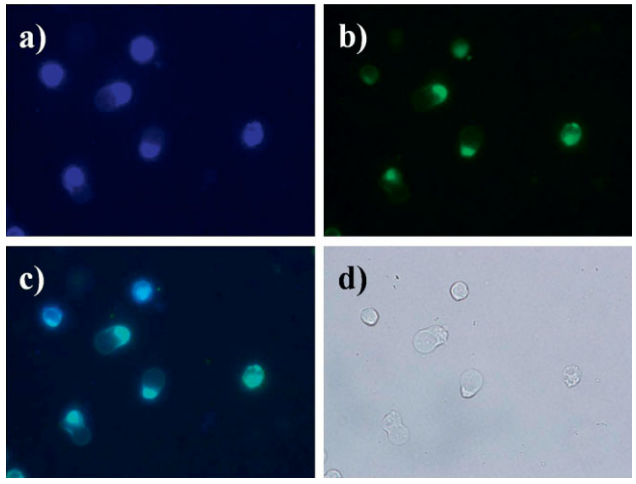


**Figure 3.** Apoptosis of Jurkat T cells induced by camptothecin (10 μM) for 4 h. The cells were costained with a) 1·2Zn (10 μM) and b) AnxV–FITC (10 μM). c) Merged image of (a) and (b). d) Phase-contrast image of the same cells.

because of the rapid loss of membrane integrity, and therefore they show the maximum fluorescence response (blue circle) to RSNPpbZn(II)–DPA.[16] On the other hand, apoptotic cells maintain the integrity of their plasma membrane (at least initially) and show relatively weaker fluorescence response (red circle) to RSNPpbZn(II)–DPA because RSNPpbZn(II)–DPA can bind only to externalized PS. The above-mentioned result strongly supports our hypothesis that RSNPpbZn(II)–DPA can selectively detect apoptotic cells.

Finally, we investigated the cellular distribution of RSNPpbZn(II)–DPA by fluorescence microscopy. After the induction of apoptosis by camptothecin for 30 min, the Jurkat T cells were treated with RSNPpbZn(II)–DPA and rinsed with culture media. As shown in Figure 6, cells that were not treated by camptothecin were not stained (Figure 6a). However, apoptotic cells in camptothecin-treated media were selectively stained with RSNPpbZn(II)–DPA (Figure 6b). Further, confocal microscopy analysis revealed that the staining was restricted to the exterior cell membrane and RSNPpbZn(II)–DPAs were localized on the cell surface, as expected if

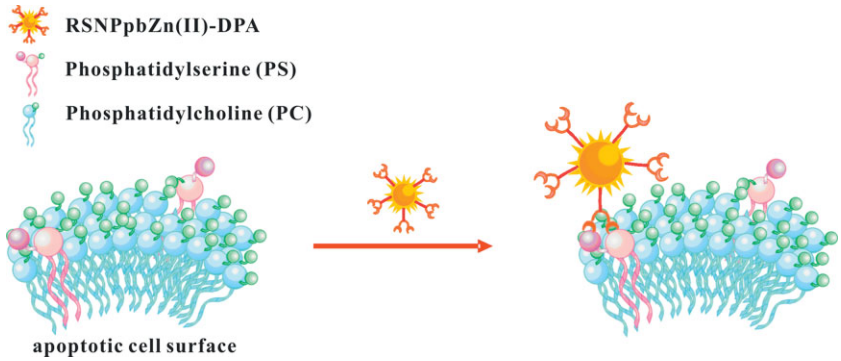


**Scheme 1.** Schematic representation of RSNPpbZn(II)–DPA and the detection of PS on a phospholipid-rich cell surface.

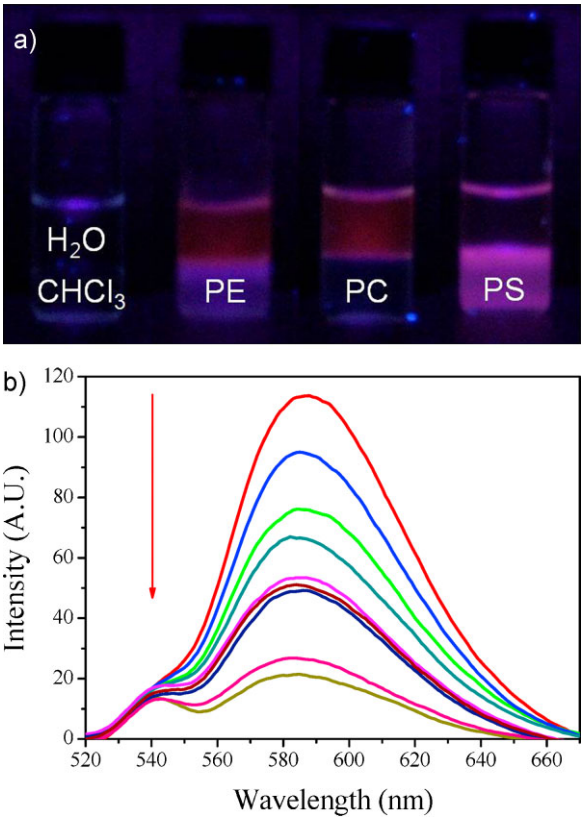


Figure 4. a) Distribution of RSNPpbZn(II)–DPA in various phospholipid solutions. RSNPpbZn(II)–DPA (50 μg mL$^{-1}$) was dissolved in HEPES buffer. In each vial, the upper layer contains the HEPES buffer and the lower layer consists of (from left to right): control, 20 mM PE in $CHCl_3$, 20 mM PC in $CHCl_3$, and 20 mM PS in $CHCl_3$ under UV light. b) Change in fluorescence intensity with increase in PS concentration. After excitation at 458 nm, the fluorescence of aqueous layer at different concentrations of PS (0, 1, 5, 25, 50, 75, 100, 250, and 500 μM) in $CHCl_3$ was measured.

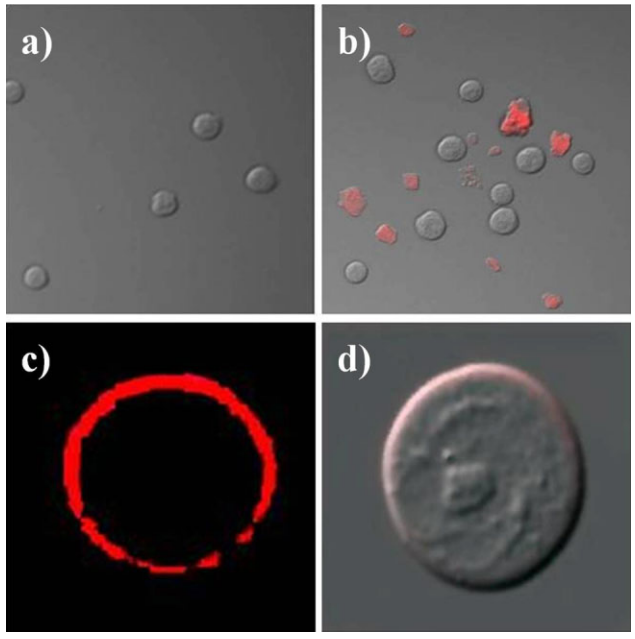


Figure 6. Microscopic images of Jurkat T cells stained with RSNPpbZn(II)–DPA: a) not treated with camptothecin and b) treated with camptothecin (30-min incubation). c) Confocal images of camptothecin-treated (30-min incubation) Jurkat T cells stained with RSNPpbZn(II)–DPA and d) the merged image of (c) and a phase-contrast image of the same cell.

the RSNPpbZn(II)–DPAs were to be bound to externalized PS (Figure 6c and d).

In summary, our results imply that pbZn(II)–DPA selectively binds to PS in preference to other phospholipids such as PC, PE, and SM. Hence, it can be used to distinguish between solutions containing different amounts of PS and other phospholipids. Furthermore, RSNPpbZn(II)–DPAs successfully bind to PS of apoptotic cells and are positioned locally on the cell surface. Specifically, our data show that RSNPpbZn(II)–DPAs can be useful in various applications, such as apoptosis imaging and cell sorting, and can help to provide an improved understanding of the interactions between cell surfaces and the surrounding materials. This approach is expected to be relevant to various biomedical applications and assessment of anticancer therapy.

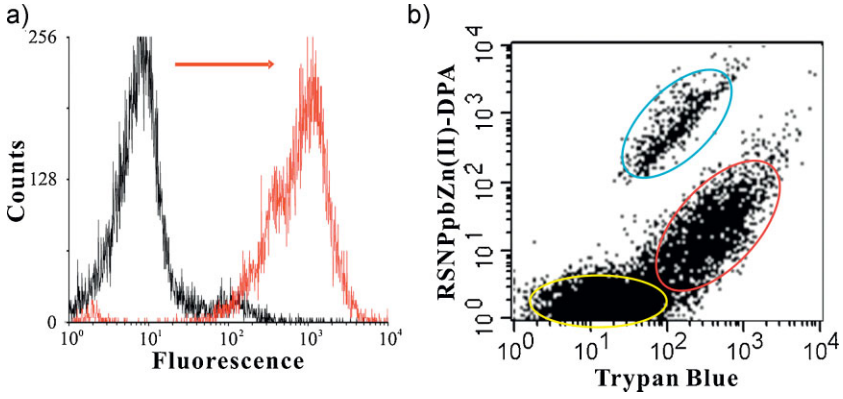


Figure 5. a) FACS analysis of Jurkat T cells with RSNPpbZn(II)–DPA: untreated (black line) and treated with camptothecin (10 μM) for 4 h (red line). b) After incubation with camptothecin (10 μM) for 30 min, Jurkat T cells were treated with RSNPpbZn(II)–DPA and also stained with trypan blue. The blue circle indicates the population of dead cells, the red circle indicates the population of apoptotic cells, and the yellow circle indicates the population of living cells. (*x* axis: fluorescence intensity of Trypan blue; *y* axis: fluorescence intensity of RSNPpbZn(II)–DPA).

## Experimental Section

*Vesicle preparations:* All lipids were purchased from Sigma-Aldrich, Inc., and stored as stock solutions in $CHCl_3$ at −20°C. Lipids were added in appropriate ratios to round-bottom flasks. The solvent was removed by rotary evaporation and the residual solvent was removed by vacuum evaporation for 2 h. The dried lipids were rehydrated in HEPES buffer (10 mM, pH 7.4) and the flasks were then vortexed vigorously. The resulting lipid dispersion was then filtered more than 20 times through a polycarbonate membrane with a pore diameter of 200 nm. All vesicles were prepared at room temperature and used the same day.

*Fluorescence spectroscopy:* Fluorescence spectroscopy was performed on a Jasco FP-6500 spectrofluorometer with Spectra Manager software (FP-6500 control driver) and by using $1 \times 1 \times 5\,cm^3$ cuvettes. All measurements were performed at 25°C without degassing the samples.

*Cell culture:* Jurkat T cells (clone E6-1) were grown in an RPMI 1640 medium containing 10% fetal bovine serum, which was changed every ≈2–3 days. Apoptosis was induced by the addition of camptothecine (1 mM in dimethyl sulfoxide (DMSO) stock) to the culture medium (total concentration: 10 μM) for 30 min or 4 h. Induction of apoptosis was verified by staining propidium iodide and AnxV–FITC in a calcium-containing buffer (BB; 1.8 mM $CaCl_2$, 10 mM HEPES, 150 mM NaCl, 5 mM KCl, 1 mM $MgCl_2$, pH 7.4). Cells were analyzed with a FACS Calibur (Becton Dickinson) by following the manufacturer's manual.

*Fluorescence microscopy:* After the incubation of all reagents, 10 μL of the cell suspension was placed on a slide and mounted on an Axiovert 200 microscope (Carl Zeiss) or a confocal laser-scanning microscope (FV-1000 Spectral, Olympus) to obtain confocal laser-scanning images.

**Keywords:**
apoptosis · cell imaging · dye-doped silica nanoparticles · phosphatidylserine

[1] a) C. B. Tompson, *Science* **1995**, *267*, 1456–1462; b) M. O. Li, M. R. Sarkisian, W. Z. Mehal, P. Rakic, R. A. Flavell, *Science* **2003**, *302*, 1560–1563.
[2] a) R. De Simone, M. Ajmone-Cat, L. Minghetti, *Mol. Neurobiol.* **2004**, *29*, 197–212; b) H. Okada, T. W. Mak, *Nat. Rev. Cancer* **2004**, *4*, 592–603.
[3] a) K. Bullok, D. Piwnica-Worns, *J. Med. Chem.* **2005**, *48*, 5404–5407; b) K. Kim, M. Lee, H. Park, J.-H. Kim, S. Kim, H. Chung, K. Choi, I.-S. Kim, B. L. Seong, I. C. Kwon, *J. Am. Chem. Soc.* **2006**, *128*, 3490–3491; c) H. Xiao, L. Liu, F. Meng, J. Huang, G. Li, *Anal. Chem.* **2008**, *80*, 5272–5275.
[4] a) D. D. Schlaepfer, T. Mehlman, W. T. Burgess, H. T. Haigler, *Proc. Natl. Acad. Sci. USA* **1987**, *84*, 6078–6082; b) R. Kaplan, M. Jaye, W. H. Burgess, *J. Biol. Chem.* **1988**, *263*, 8037–8043; c) G. Koopman, C. P. Reutelingsperger, G. A. M. Kuijten, *Blood* **1994**, *84*, 1415–1420; d) I. Vermes, C. Haanen, H. Steffens-Nakken, C. Reutelingsperger, *J. Immunol. Methods* **1995**, *184*, 39–51.
[5] a) J. A. F. Op den Kamp, *Annu. Rev. Biochem.* **1979**, *48*, 47–71; b) J. M. Boon, B. D. Smith, *Med. Res. Rev.* **2002**, *22*, 251–281.
[6] R. A. Schlegel, P. Williamson, *Cell Death Differ.* **2001**, *8*, 551–563.
[7] a) M. van Engeland, L. J. Nieland, F. C. Ramaekers, B. Schutte, C. P. Reutelingsperger, *Cytometry* **1998**, *31*, 1–9; b) B. Plasier, D. R. Lloyd, G. C. Paul, C. R. Thomas, M. Al Rubeai, *J. Immunol. Methods* **1999**, *229*, 81–95; c) P. Williamson, S. van den Eijnde, R. A. Schlegel, *Methods Cell Biol.* **2001**, *66*, 339–365.
[8] K. Balasubramanian, E. M. Bevers, G. M. Willems, A. J. Schroit, *Biochemistry* **2001**, *40*, 8672–8676.
[9] a) V. A. Fadok, D. L. Bratton, D. M. Rose, A. Pearson, R. A. B. Ezekewitz, P. M. Henson, *Nature* **2000**, *405*, 85–90; b) S. J. Martin, C. P. Reutelingsperger, A. J. McGahon, J. A. Rader, R. C. van Schie, D. M. LaFace, D. R. Green, *J. Exp. Med.* **1995**, *182*, 1545–1556.
[10] a) J. Y. Lee, S. Miraglia, X. W. Yan, E. Swartzman, S. Cornell-Kennon, J. Mellentin-Michelotti, C. Brusco, D. S. France, *J. Biomol. Screening* **2003**, *8*, 81–88; b) J. A. Barmes, A. V. Gomes, *Mol. Cell. Biochem.* **2002**, *231*, 1–7.
[11] a) A. V. Koulov, K. A. Stucker, C. Lakshmi, J. P. Robinson, B. D. Smith, *Cell Death Differ.* **2003**, *10*, 1357–1359; b) R. G. Hanshaw, B. D. Smith, *Bioorg. Med. Chem.* **2005**, *13*, 5035–5042; c) K. M. DiVittorio, J. R. Johnson, E. Johansson, A. J. Reynolds, K. A. Jolliffe, B. D. Smith, *Org. Biomol. Chem.* **2006**, *4*, 1966–1976; d) A. Ojida, Y. Mito-Oka, K. Sada, I. Hamachi, *J. Am. Chem. Soc.* **2004**, *126*, 2454–2463; e) L. Quinti, R. Weissleder, C.-H. Tung, *Nano Lett.* **2006**, *6*, 488–490; f) R. G. Hanshaw, C. Lakshmi, T. N. Lambert, J. R. Johnson, B. D. Smith, *ChemBioChem* **2005**, *6*, 2214–2220.
[12] A. Malyguine, E. Derby, A. Brooks, V. Reddy, M. Baseler, T. Sayers, *Immunol. Lett.* **2002**, *83*, 55–59.
[13] a) D. H. Lee, J. H. Im, S. U. Son, Y. K. Chung, J.-I. Hong, *J. Am. Chem. Soc.* **2003**, *125*, 7752–7753; b) D. H. Lee, S. Y. Kim, J.-I. Hong, *Angew. Chem. Int. Ed.* **2004**, *43*, 4777–4780; c) J. H. Lee, J. Park, M. S. Lah, J. Chin, J.-I. Hong, *Org. Lett.* **2007**, *9*, 3729–3731; d) S. K. Kim, D. H. Lee, J.-I. Hong, J. Yoon, *Acc. Chem. Res.* **2009**, *42*, 23–31; e) H. W. Rhee, S. J. Choi, S. H. Yoo, Y. O. Jang, H. H. Park, R. M. Pinto, J. C. Cameselle, F. J. Sandoval, S. Roje, K. Han, D. S. Chung, J. Suh, J.-I. Hong, *J. Am. Chem. Soc.* **2009**, *131*, 10107–10112; f) Y. S. Kim, H. H. Park, H. W. Rhee, J.-I. Hong, K. Han, *Ann. Clin. Lab. Sci.* **2009**, *39*, 114–119.
[14] a) W. Tan, K. Wang, X. He, X. J. Zhao, T. Drake, L. Wang, R. P. Bagwe, *Med. Res. Rev.* **2004**, *24*, 621–638; b) L. Wang, W. Zhao, W. Tan, *Nano Res.* **2008**, *1*, 99–115.
[15] a) H. J. Phillips, J. E. Terryberry, *Exp. Cell. Res.* **1957**, *13*, 341–347; b) R. D. Lillie, *Conn's Biological Stains*, 9thEd. Williams and Wilkins, Baltimore **1977**, p. 158.
[16] K. L. Rock, H. Kono, *Annu. Rev. Pathol.* **2008**, *3*, 99–126.

Received: April 7, 2010

  